TECHNICAL MEMORANDUMS

NATIONAL ADVISORY COMMITTEE FOR AERONAUTICS

No. 784

TORSION AND BUCKLING OF OPEN SECTIONS

By H. Wagner and W. Pretschner

Luftfahrtforschung
Vol. XI, No. 6, December 5, 1934
Verlag von R. Oldenbourg, Munchen und Berlin

Washington
January 1936

NATIONAL ADVISORY COMMITTEE FOR AERONAUTICS

TECHNICAL MEMORANDUM NO. 784

TORSION AND BUCKLING OF OPEN SECTIONS*

By H. Wagner and W. Pretschner

SUMMARY

Following an abstract of the well-known theory of torsion in compression, the writers give directions for the practical calculation of the values of C_{BT} (resistance to flexure and torsion) and i_{SP}^2, which determine the torsion.

The second part treats the experiments in support of the theory of torsion of plain and flanged angle sections. The experiments are in quite close agreement with the original theory (omission of elastic deflection). The existing minor discrepancies are conclusively explained through the subsequent modification of the theory (allowance for elastic deflections). Under eccentric compressive stresses, long buckling struts are particularly subject to great deformations in the median zone, which produce a change in sectional stress distribution over the length of the member. The scope of application of the theory is extended to include long eccentrically compressed members by introducing a theoretically established mean value for the load eccentricity along length $f_m = 0.85\ f_{max}$.

After this extension the experiments with flanged angle sections are remarkably close to the theory. On the other hand, since the discrepancies between the original and the modified theory average only about 10 percent for the longest test specimens, and the application of the original theory still affords a small safety margin, its use commends itself for general purposes.

For the plain (nonflanged) angle sections the original theory revealed a much closer agreement than the modified theory. But nonflanged sections form an exception among all other sections: Their resistance to flexure and torsion

---

*"Verdrehung und Knickung von offenen Profilen." Luftfahrtforschung, December 5, 1934, pp. 174-180.

C_{BT}, is abnormally low compared to the torsipnal stiffness; that is, the buckling load is almost independent of the length of the deformation. So when the direction of the eccentricity is favorable for the median zone of the member, these sections are subject to local deformations at the ends.

I. INTRODUCTION

Open sections are members drawn or rolled from strip which, in contrast to the closed (tubular) sections, enclose no hollow space. The former have a very low torsional stiffness compared to the latter. Thus the torsional stiffness of an open section drawn from strip whose cross-sectional warping is not prevented, is exactly as great as that of the flat strip from which it was made. But, if the warping of the cross section is prevented, say, at one end of the member, longitudinal stresses are developed which offer considerable resistance against torsion when the member is relatively short.

When used as a compression member, such a section fails frequently by twisting long before the Eulerian buckling load or the yield point has been reached. This twisting failure of the strut reverts, for centrically loaded members, to a simple stability problem and is similar to the torsional instability of beams subjected to bending.

II. TORSION OF OPEN SECTIONS WITH CROSS SECTION RESTRAINED AGAINST WARPING

This condition is illustrated in figure 1. It is seen that in the twisted attitude the points at the end surfaces originally in a plane (as well as all other cross-sectional surfaces) have shifted from the original plane according to the displacement ξ.

The difference $\Delta\xi$ between the displacement of points 1 and 2 amounts to

$$\Delta\xi = \frac{\varphi}{x} r_u \Delta u = \vartheta r_u \Delta u = 2 \Delta F \vartheta \qquad (1)$$

where x = length of section, respectively, coordinate in longitudinal direction.

φ = angle of torsion.

$\vartheta = \frac{\varphi}{x}$, respectively, $\frac{d\varphi}{dx} = \varphi' =$ angle of twist per unit length.

$\Delta F = \frac{1}{2} r_u \Delta u =$ area enclosed by the radius vectors from the axis of rotation to points 1 and 2 and by the "part of the periphery" Δu.

For an open section of any cross-sectional form which is twisted about its axis of rotation S, it is

$$\xi = 2F \vartheta$$

where $F = \Sigma \frac{1}{2} r_u \Delta u$, area between the radius vectors through S and the periphery of the section. One radius vector goes to the point, whose longitudinal displacement (arbitrary for the present) = 0, the other to the point for which the displacement (fig. 2) is desired. When defining the displacement for point 4 (fig. 3), the difference $F_1 - F_2$ must be substituted for F.

The displacement is proportional to ϑ; for $\vartheta = 1$, it is called "unit displacement" and designated with the letter w. Thus,

$$w = 2F \quad \text{and} \quad \xi = w \vartheta$$

Open sections stressed in torque are subject to longitudinal stresses when clamped at one end. The I-section shown in figure 4 is under a torque load $Q h = M$. The longitudinal stresses are also shown. Their distribution over the section is precisely as that of the displacement produced with unrestrained torsion

$$\sigma = \text{proportional to } w$$

This is readily understood when observing that for uniform torsion, ϑ = constant, the section exhibits, according to equation (1), identically great warping in all cross sections, i.e., that the longitudinal fibers of the section experience no length changes. Variable ϑ is followed by displacements ξ variable along the length. This

induces linear elongations in the longitudinal fibers of the section

$$\epsilon = \frac{d\xi}{dx}$$

or, according to (1) the stresses:

$$\sigma = E\,\epsilon = E\,\frac{d\xi}{dx} = E\,w\,\frac{d\vartheta}{dx} = E\,w\,\frac{d^2\varphi}{dx^2} \qquad (2)$$

The work of form change affords the best means for studying the relationship between the outside torque M and the longitudinal stresses. The moment applied at the tip of the beam producing angle of torsion φ performs the work $\frac{1}{2}\,M\,\varphi$, which must equal the work of the longitudinal stresses or:

$$\frac{1}{2}\,M\,\varphi = \frac{1}{2E}\int^{V}\sigma^2\,dV = \frac{1}{2E}\int^{V}E^2\,w^2\left(\frac{d^2\varphi}{dx^2}\right)^2 dx\,dF =$$

$$= \frac{E}{2}\int^{F}w^2\,dF\int_0^{l}\left(\frac{d^2\varphi}{dx^2}\right)^2 dx$$

It is seen that the resistance against the torsion moment is proportional to a quantity:

$$\int^{F}w^2\,dF = C_{BT} \qquad (3)$$

This value represents the so-called "torsion-bending constant."

Integration along x affords the relation*

$$M_B\,l = \frac{C_{BT}}{w}\,\sigma \quad \text{that is,} \quad \sigma = \frac{M\,l}{C_{BT}}\,w \qquad (4)$$

$$M_B = -\,E\,C_{BT}\,\frac{d^3\varphi}{dx^3} \qquad (5)$$

With allowance for the temporarily disregarded Saint-Venant's torsional stiffness $G\,J_T$, it is

$$M = -\,E\,C_{bd}\,\frac{d^3\varphi}{dx^3} + G\,J_T\,\frac{d\varphi}{dx} \qquad (6)$$

---

*These equations are in strict accord with the relations of the theory of flexure:

$P\,l = \frac{J}{\eta}\,\sigma$; whereby $J = \int \eta^2\,dF$ and $P = EJ\,\frac{d^3y}{dx^3}$

III. TWISTING FAILURE OF STRUTS

When stressing a comparatively thin-walled open section, such as an angle section in compression, each individual flange tends to buckle at right angles to its plane (fig. 5). But the side of the flange lying at the corner of the angle section supports itself against the other flange which, in view of such stresses, has a very high section modulus and consequently prevents the buckling of the first flange at this point and vice versa.

Thus, we have two possible forms of buckling:

1) both flanges buckle in the same direction - the section is rotated as a whole by twisting (fig. 5a);

2) both flanges buckle in opposite directions (fig. 5b).

With the latter type of buckling the angle section is deformed, as a result of which the work of form change is greater in this case. On the other hand, of the two possible forms of buckling, the one invariably occurs first to which the least work of form change corresponds for equal work of the outside loads, i.e., twisting of the section.

Now we discuss the general case. An originally straight, open section is under a sensibly eccentrically acting compressive stress P, whose line of action is parallel to the strut axis. $\sigma_D = \frac{P}{F}$ is to denote the mean compressive stress, and σ_P the assumedly predetermined resultant compressive and bending stress variable across the section. The σ_P stresses run in direction of the longitudinal fibers of the section; that is, they slope obliquely to the original axis as the section is distorted. The angle of inclination of a fiber due to torsion is $r\,\varphi'$. Thus $\sigma_P\, r\, \varphi'$ is the horizontal component of σ_P; its direction is perpendicular to r. These stresses set up a moment about the center of shear amounting to

$$M_{P\varphi} = \varphi' \int^{F} r^2\, \sigma_P\, dF =$$

$$= \varphi'\, \sigma_D \int^{F} \frac{\sigma_P}{\sigma_D}\, r^2\, dF = \varphi'\, P\, i_{SP}^2 \qquad (7)$$

where $$\frac{1}{F}\int \frac{\sigma_P}{\sigma_D} r^2 \, dF = i_{SP}^2 \qquad (7a)$$

For centrically acting force P, we have $\sigma_P = \sigma_D$; that is, $M_{P\varphi} = \varphi' \, \sigma_{P_o} \, J_s$, with J_s = polar moment of inertia of profile section about the axis of shear.

Dividing $\sigma_P = \sigma_D + \sigma_B$ into the quota of pure compression and bending stress due to eccentricity e of the compressive strain, we have:

$$i_{SP}^2 = \frac{1}{F}\int \frac{\sigma_D + \sigma_B}{\sigma_D} r^2 \, dF = \frac{1}{F}\int r^2 \, dF + e\frac{1}{J}\int \eta \, r^2 \, dF$$

$$i_{SP}^2 = i_S^2 + e \, i_\eta \qquad (8)$$

with η = distance of surface particle dF from the neutral axis, and J = moment of inertia of the section; i_S^2 and i_η are section constants.

The moment $M_{P\varphi}$ is, according to (6) in equilibrium with the moment of the shearing stresses, so that the differential equation for torsion becomes:

$$\varphi''' \, E \, C_{BT} + \varphi' \, (P \, i_{SP}^2 - G \, J_T) = 0 \qquad (9)$$

The solution for the most important case, i.e., cross-sectional warping not restrained at the ends, is:

$$\varphi = \varphi_o \sin \frac{\pi x}{L} \quad (\varphi_o = \text{angle of torsion in center})$$

with the limiting condition:

$$\varphi = 0 \quad \text{and} \quad \varphi'' = 0 \quad \text{for} \quad x = 0 \quad \text{and} \quad x = L.$$

Insertion in the differential equation gives the buckling load:

$$P_w = \frac{1}{i_{SP}^2}\left(G \, J_T + \frac{\pi^2}{l^2} E \, C_{BT}\right) \qquad (10)$$

If the load acting on the member is lower than the buckling load given by this equation, the member is not distorted at all, provided there is no initial distortion in the center.

But if the load reaches the amount indicated, the member gives way suddenly under the effect of the torsion (simple stability problem). Only those sections having a low value C_{BT}/i_{SP}^2 with respect to the moment of inertia of the profile section (compare equation (10)) have a tendency to fail by twisting.

There is no connection between crippling (according to Euler) and twisting for buckling struts under centrical load; the section is either to be calculated for Eulerian crippling load or twisting, depending on whether the lower buckling load corresponds to one or the other of the two phenomena.

In long, eccentrically compressed members the deflection due to eccentricity may become so great that the stress distribution in the median zone is sensibly unlike that at the ends (i_{SP}^2 is then variable along x, according to equation (9)). We shall refer to this again in a subsequent section. Formula (10) is satisfactory for most practical cases.

Yet another case is that of a member originally slightly twisted, so as to produce in the center an initial elongation through an angle φ_o. Assuming a sinusoidal torsion, the angle φ gradually increases according to the law of

$$\varphi = \frac{\varphi_o}{1 - \frac{P}{P_w}}$$

as the load increases. A gradual increase in twist occurs equally in an originally quite straight member when, for example, in a symmetrical profile section the compressive force P acts outside of the plane of symmetry. Such cases are discussed in detail in the publication printed incidental to the twenty-fifth anniversary of the Danzig Technical Institute.

IV. DETERMINATION OF THE SHEAR CENTER AND THE TORSION-BENDING CONSTANT

a) Shear Center

To prove the absence of special difficulties involved in determining the shear center and the torsion-bending constant C_{BT}, we define both hereinafter with the aid of a symmetrical cross section. The rounded-off places are replaced by identical straight parts.

For bending about the plane of symmetry of the cross section (as zero stress curve) the location of the resultant shear force is determined from the distribution of the shearing stresses. The change $\Delta \tau s$ of the shear force τs on a part Δu of the cross section is proportional to the distance y of the surface elements $s \Delta u$ from the zero stress curve (fig. 6). The proportionality factor is arbitrarily put equal to 1, thus:

$$\Delta \tau s = y s \Delta u$$

When a straight piece of the profile section is of constant wall thickness, the shearing force per unit length along this piece is parabolical. With known τs at start 1 of the straight piece, the shearing force τs_2 at point 2 and transverse force Q_{12} acting on piece 1:2 are:

$$\tau s_2 = \tau s_1 + l_{12} \frac{y_1 + y_2}{2} \tag{11}$$

$$Q_{12} = \tau s_1 l_{12} + l_{12}^2 \left(\frac{1}{3} y_1 + \frac{1}{6} y_2 \right) \tag{12}$$

Starting at one of the two section tips, the line of action of the resultant transverse force is readily obtained. The intersection of this line with the axis of symmetry is the center of shear.

b) Determination of C_{BT}

The torsion-bending constant $C_{BT} = \int_F w^2 \, dF$ is found graphically or, preferably, analytically. The "unit displacement" w varies linearly for every straight piece of

the profile periphery and is readily computable. In the plane of symmetry, we have $w = 0$. Figure 7 shows w for the flanged section with the corner areas replaced by straight lines.

With the notations of figure 7, it is:

$$C_{BT} = \int w^2 \, dF = \Sigma \, s \int (w_1 + a \, x)^2 \, dx =$$

$$\Sigma \, s \, l \left[w_1^2 + w_1 \, a \, l + \frac{1}{3} (a \, l)^2 \right] \qquad (13)$$

or, after conversion conformal, to $a \, l = w_2 - w_1$ (fig. 7):

$$C_{BT} = \frac{1}{3} \Sigma \, s \, l \, (w_1^2 + w_2 + w_2^2) \qquad (14)$$

It can be proved* that w consists of two parts: $w = w_u + w_n$, heretofore expressed with $w \doteq w_u$ and, accordingly, $C_{BT_u} \doteq C_{BT}$, because w_n is of secondary significance with the conventional thin-walled structures employed in airplane design. Thus, aside from the calculated $C_{BT} \doteq C_{BT_u}$ there is yet C_{BT_n}, which may be expressed with a simple integral. With the notations of figure 8, it is:

$$C_{BT_n} = \frac{s^3}{12} \int^u r_n^2 \, d_n = \frac{s^3}{12} \int^u r_n^2 \, dr_n \qquad (15)$$

V. EXPERIMENTAL RESULTS

a) Test Samples

To check the theoretical loads for twisting failure, we made a number of buckling tests on open compression members. The results show a very close agreement with the calculation. In order to obtain a clear picture of the effect of each quantity appearing in

$$P_w = \frac{1}{i_{SP}^2} \left(G \, J_T + \frac{\pi^2}{l^2} E \, C_{BT} \right)^{**} \qquad (10)$$

---

*25th anniversary number of the Danzig Technical Institute, p. 331.

**See equation (10), warping not restrained.

two profile sections of drawn dural strip of equal cross-sectional area ($F = 0.56$ cm^2) and shank length (2.9 cm) were chosen (fig. 9).

The buckling loads were determined through experiments with three different lengths ($l = 18.6$; $l = 38.6$; and $l = 58.6$ cm) with respect to the eccentricity of the load applied at the plane of symmetry.

The profile constants computed from exact measurements are given in the following:

TABLE I

	Notation	Dimension	Section shape C	Section shape <
Cross-sectional area	F	cm^2	0.565	0.566
Wall thickness	s	cm	.085	.10
Length of developed section	b	cm	6.64	5.66
Distance of center of gravity	x_S	cm	1.228	1.10
Distance of shear center	x_{Sch}	cm	.137	.0326
Moment of inertia about axis x	J_x	cm^4	.955	.885
Moment of inertia about axis y	J_y	cm^4	.275	.198
Polar moment of inertia about shear center	J_P	cm^4	2.273	1.700
Torsion-bending constant	C_{BT}	cm^6	.060	.0016
Constant	i_S^2	cm^2	4.02	3.00
Constant	i_η	cm	4.44	4.20
Modulus of elasticity	E	kg/cm^2	740000	740000
Torsional stiffness	G J_T	kg/cm^2	400	405

cm x 0.3937 = in.; cm^2 x 0.1550 = sq.in.; kg/cm^2 x 14.2235 = lb./sq.in.

b) Test Arrangement

The loading machine employed in the tests is illustrated in figure 10.

The bar (a) is compressed between two sets of crossed knife edges (g). The load is applied at the end of a lever by means of weights (d). The buckling load was determined with an accuracy of ±0.3 kg.

The eccentricity of the compressive load was determined through measuring the deflection during the loading and the initial eccentricity was derived therefrom. This removed the unavoidable errors incident to direct determination of initial eccentricity and the effect of any initial deformation.

The deflection, measured with a solid rod (f) on two knife edges and micrometer screw (m), was accurate to within ±0.02 mm.

The modulus of elasticity and the torsional stiffness were determined from careful tension and torsion tests.

c) Centrically Compressed Members

$$P_w = \frac{1}{i_{SP}^2}\left(G\,J_T + \frac{\pi^2}{l^2}\,E\,C_{BT}\right)$$

$$i_{SP}^2 = \frac{1}{F}\int r^2\,dF = \text{constant} = i_S^2 \qquad (10a)$$

For this case figures 11 and 12 show, aside from the torsion loads (stresses), the Euler curves for both sections with respect to length and slenderness ratio. The respective proportion of $G\,J_T$ and C_{BT} to the quantity of the torsion load is also included.

Both sections have exceeded the stability limit with regard to torsion stress long before the Eulerian load is reached. The short bar of flanged section is appreciably superior to the angle section because of its high C_{BT}, but as the length increases the effect of C_{BT} becomes small compared to $G\,J_T$. For long bars, the torsional stiffness practically governs the torsion load, and for this reason the angle section is superior to the flanged section.

kg × 2.20462 = lb.; mm × 0.03937 = in.

The measured torsion loads are shown as points. Up to the result for angle section of $l = 18.6$ cm the test data (of very close accuracy for buckling tests) are in accord with the calculation.

The discrepancy in this case ($l = 18.6$ cm) may be attributed to the restraint of the end cross sections against warping through w_n. (See footnote (*), p. 9.) Allowing for this fact the results are as shown by the dot-dash curves of figure 12. (With complete restraint of the end cross sections against warping the value of C_{BT} is four times as high.)

d) Eccentrically Compressed Members

$$P_w = \frac{1}{i_S^2 + i_\eta e}\left(G J_T + \frac{\pi^2}{l^2} E C_{BT}\right) \qquad (10b)$$

The results are illustrated in figures 13 to 18. Eccentricity from the center of gravity toward the back of the section is figured negative. The ratio of effective torsion load P_w to the torsion load P_{w_o} of the centrically compressed bar chosen as criterion affords a more comprehensive comparison.

These curves reveal the intimate relationship between torsion load and load eccentricity. If the load acts in the vicinity of the shear center the torsion load finally becomes infinitely great. With $P_w \rightarrow$ infinite, i.e., $i_{SP}^2 \rightarrow 0$ (compare also equation (8)), the corresponding eccentricity is, according to (10):

$$\lim_{P \rightarrow \infty} e = -\frac{i_S^2}{i_\eta} \qquad (16)$$

The dashed theoretical curves are computed for assumedly constant stress distribution. (See fig. 19; $\sigma_P = \sigma_D + \sigma_B$ is constant in every section over the whole length of the member.)

But under eccentric stress the strut deflects (column effect); thus the eccentricity, and consequently, the stress distribution over the length of the bar becomes variable (fig. 20). Taking into consideration the thus-obtained

exact stress distribution (considerable paper work involved) the full lines represent the torsion loads.*

It is seen that all major discrepancies (from 10b) are practically confined to long bars and to the range of negative eccentricity, so that as a general rule this simple calculation is close enough for estimations.

When, in long sections, the force acts in the vicinity of the corner, the deflection in the center causes the line of action in the median part of the section to shift more toward the corner. The result is a stress distribution in the center such as to void the question of twisting at this point. (See equation (16).) Thus it happens in the test that the section first has a tendency to twist, but returns to its median position as the load increases; that is, the deflection in the center increases and then breaks in a different manner. (See fig. 18, at e = - 4.0 mm.) In plain (nonflanged) sections, the increased value of the torsion load does not conform to the beneficial eccentricity in the bar center, but rather to the form as illustrated in figure 21b, where the torsion load corresponds to the eccentricity at the ends. Thus the test samples of the angle sections of length l = 58.6 cm, excepting e = - 4.0 mm, twisted according to figure 21b; all others according to figure 21a. The latter form does not appear when the section is flanged as, owing to the shorter buckling length in this case, resulting from the high C_{BT}, the buckling load would be considerably higher. (Compare the effect of l in equation (10).)

Numerically the experiments are in quite close accord with the theoretical results.

---

*Note: Let f_{max} be the maximum deflection of the bar. Then the additional stress distributed sinusoidally over the bar length may be replaced by a constant distribution having the same work of deformation if the additional eccentricity equals 0.85 f_{max}, and the calculation is reduced to case a)

If 0.85 f_{max} = n, then (according to Hütte, vol. I (25th edition), p. 645:

$$n = \frac{0.85}{\cos \frac{\pi}{2}\sqrt{\frac{P}{P_E}}} + 0.15 \quad \text{and} \quad P_w = \frac{G\,J_T + \frac{\pi^2}{l^2} E\,C_{BT}}{i_S^2 + i_\eta\, e\, n}$$

It is best to resolve this equation graphically by computing P_w/P for any P and defining P_w from $\frac{P_w}{P} = 1$.

As concerns the discrepancies, we note: The discrepancies occurring in the test with the short angle section (fig. 16) are - as for centrically loaded sections - a result of cross-sectional buckling unavoidable in the test.

Owing to inaccuracies in preparation, the profile surfaces assumed as flat in the calculation of C_{BT} were actually slightly curved. The result was that the actual C_{BT} were slightly higher than those used in the calculation, which explains the slightly higher torsion load shown for all short sections (figs. 11 and 12). This is particularly noticeable on the angle sections because of their inherently low C_{BT} values.

The mathematical deflections in the strut center are plotted for torsion load versus eccentricity and are in close agreement with the measured values.

Translation by J. Vanier,
National Advisory Committee
for Aeronautics.

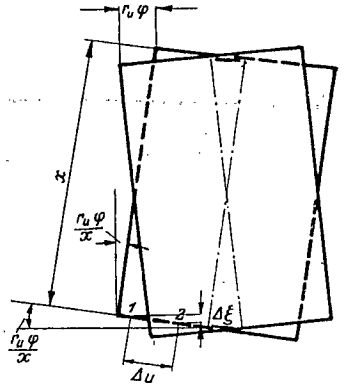

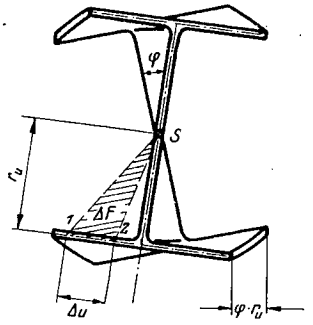

Figure 1.- Distorted I-beam.

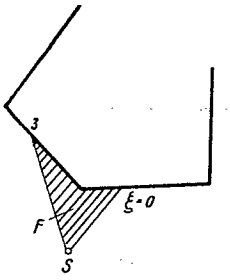

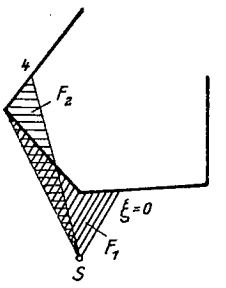

Figures 2,3.- Formation of the displacements.

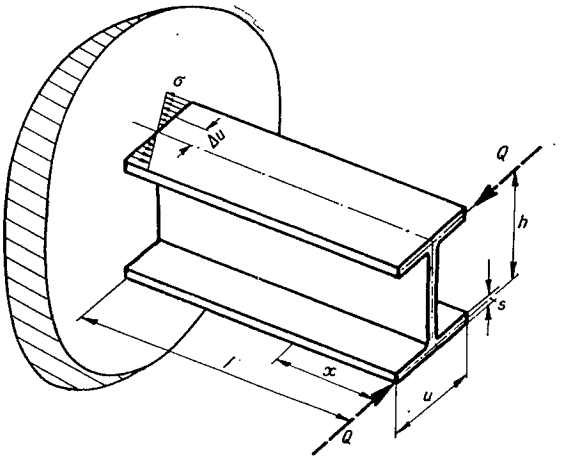

Figure 4.- Formation of longitudinal stresses with restraint of the end cross-section against warping.

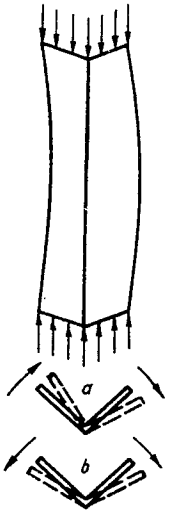

Figure 5.- Types of buckling

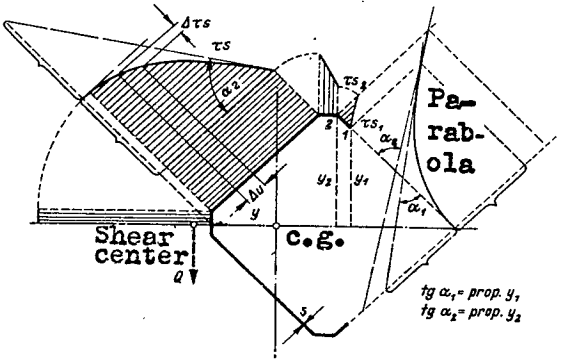

Figure 6.- Shearing stresses due to transverse force through shear center.

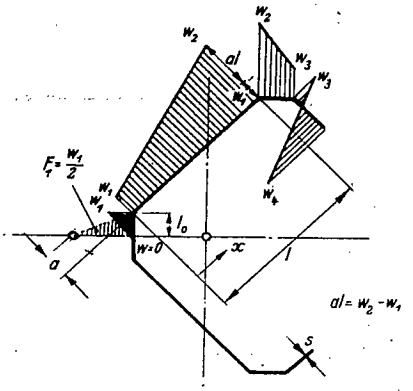

Figure 7.- Variation of the unit displacement.

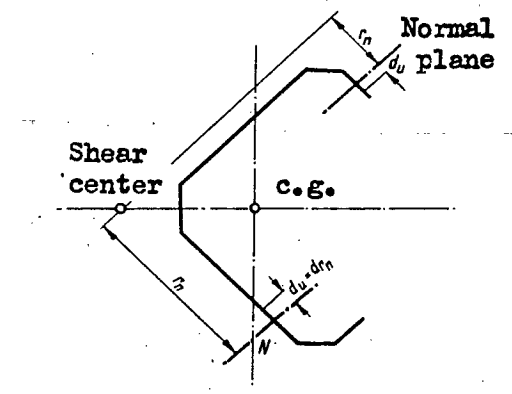

Figure 8.- Definition of C_{BT_n}

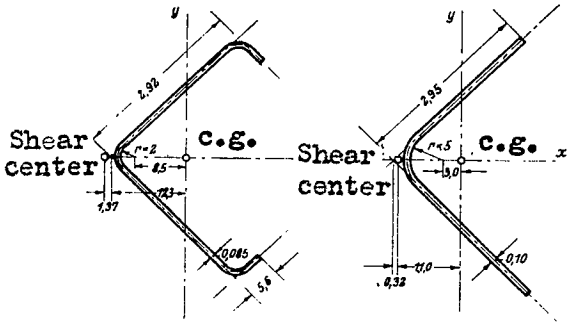

Figure 9.- Dimensions of examined sections.

Figure 10.- Loading machine.

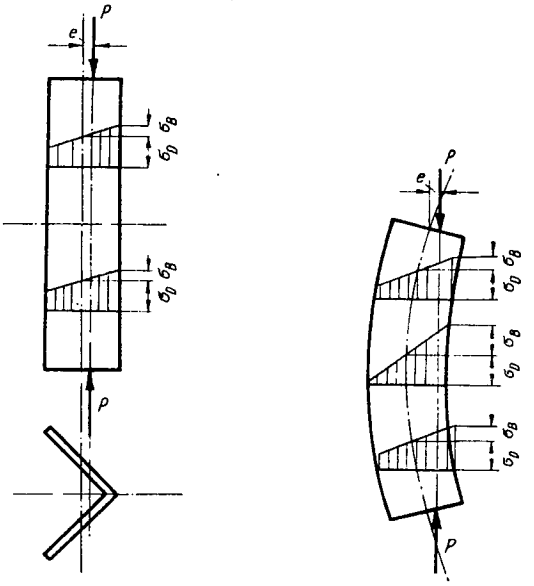

Figures 19,20.- Modified and actual stress distribution in eccentric compression.

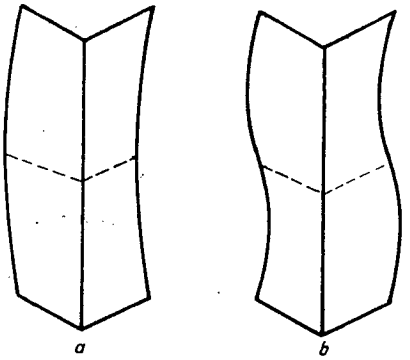

Figure 21.- Forms of torsion of open sections.

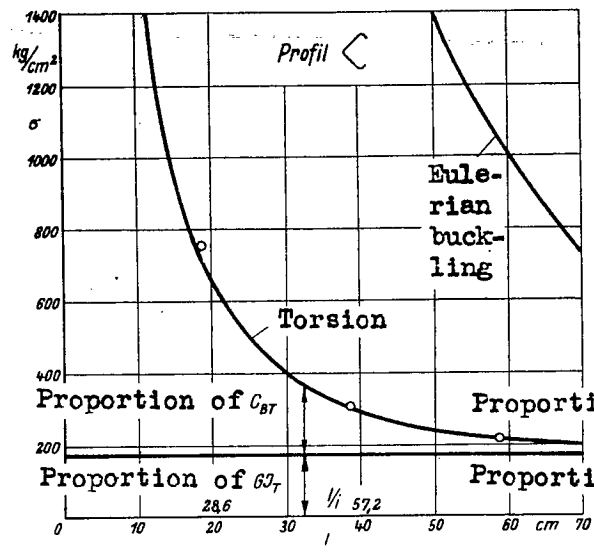

Figure 11.

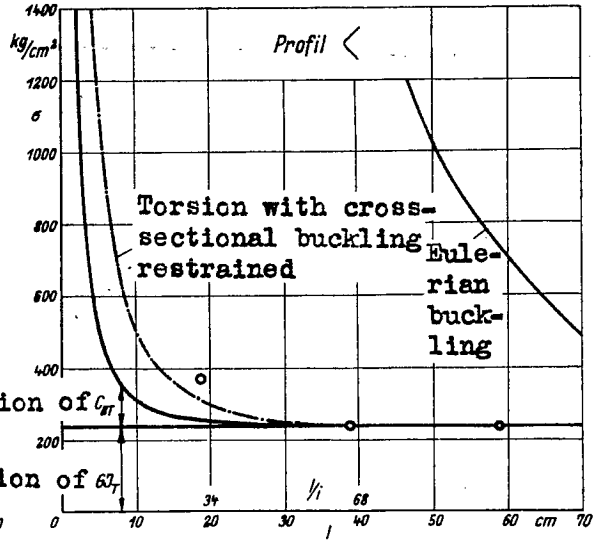

Figure 12.

Figures 11,12.- Torsion loads in centrical compression.

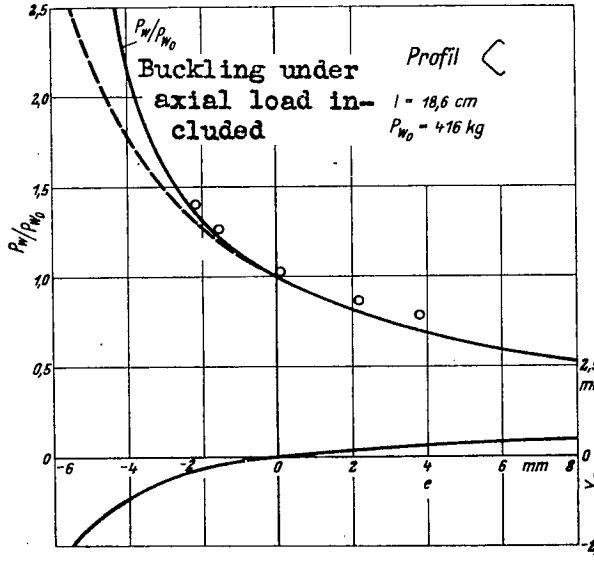

Figure 13.

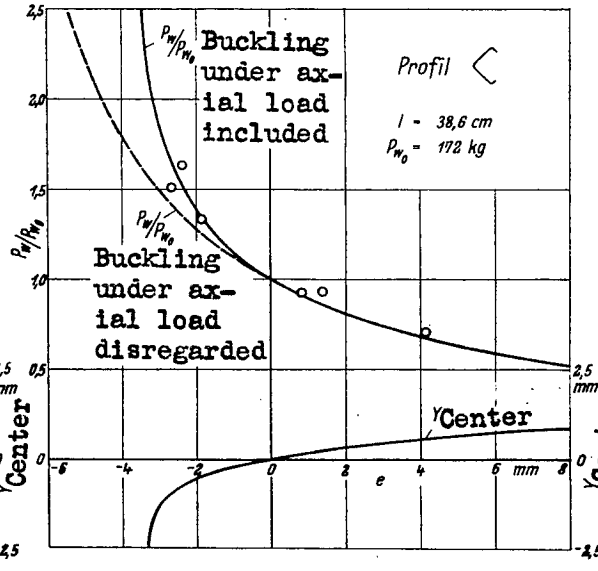

Figure 14.

Figures 13,14.- Ratio of torsion loads in eccentric to centric compression.

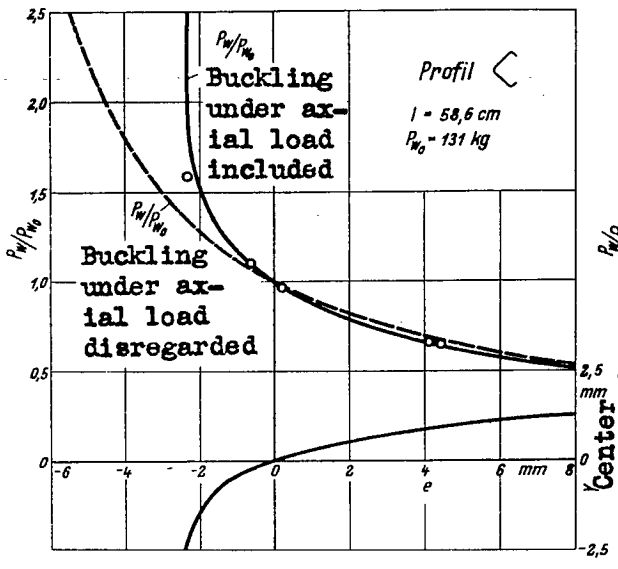

Figure 15.

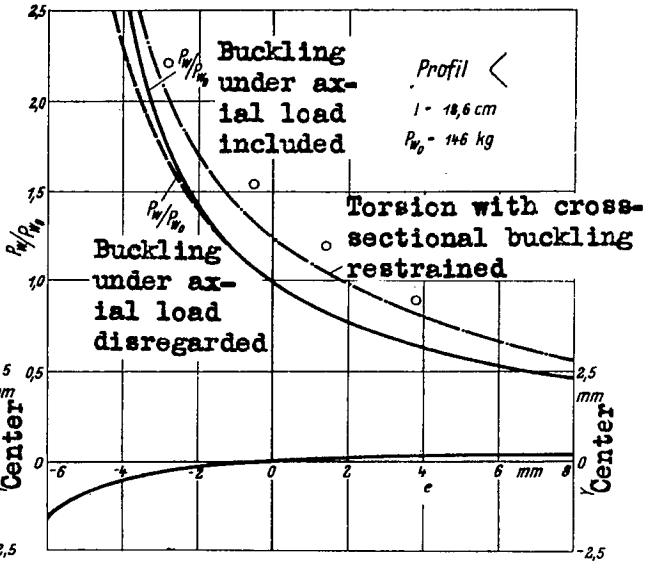

Figure 16.

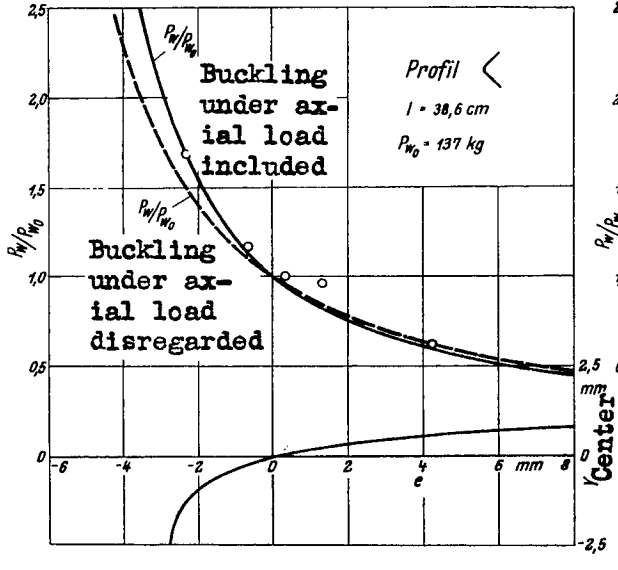

Figure 17.

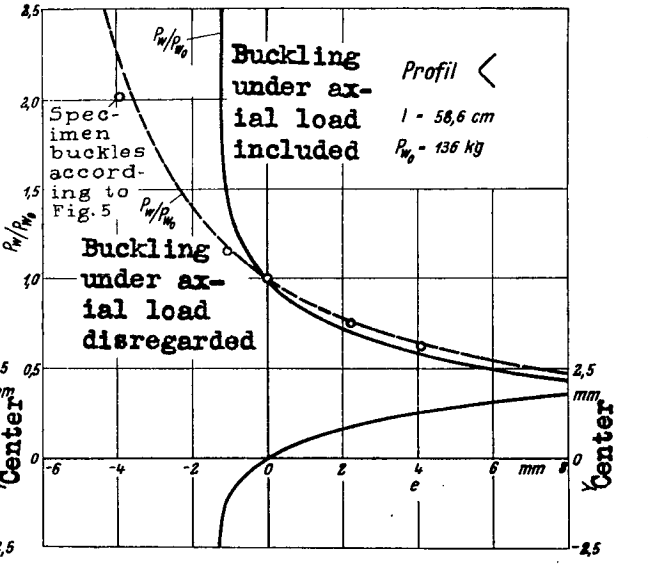

Figure 18.

Figures 15,16,17,18.- Ratio of torsion loads in eccentric to centric compression.